Inorg. Chem. **2004**, *43*, 4846–4861

Mechanism of Abstraction Reactions of Dimetallenes ($R_2X{=}XR_2$; X = C, Si, Ge, Sn, Pb) with Halocarbons: A Theoretical Study

Ming-Der Su*

School of Medicinal and Applied Chemistry, Kaohsiung Medical University, Kaohsiung 80708, Taiwan, ROC

Received December 10, 2003

Potential energy surfaces for the abstraction reactions of dimetallenes with halocarbons have been studied using density functional theory (B3LYP). Five dimetallene species, $(SiH_3)_2X{=}X(SiH_3)_2$, where X = C, Si, Ge, Sn, and Pb, have been chosen in this work as model reactants. The present theoretical investigations suggest that the relative dimetallenic reactivity increases in the order C=C ≪ Si=Si < Ge=Ge < Sn=Sn < Pb=Pb. That is to say, for halocarbon abstractions there is a very clear trend toward lower activation barriers and more exothermic reactions on going from C to Pb. Moreover, for a given dimetallene, the overall barrier heights are determined to be in the order $CF_4 > CCl_4 > CBr_4 > CI_4$. That is, the heavier the halogen atom (Y), the more facile its abstraction from CY_4. Halogen abstraction is always predicted to be much faster than the abstraction of a CY_3 group irrespective of the dimetallene or halocarbon involved. Our model conclusions are consistent with some available experimental findings. Furthermore, both a configuration mixing model based on the work of Pross and Shaik and bonding dissociation energies can be used to rationalize the computational results. These results allow a number of predictions to be made.

I. Introduction

Since the first presentation of firm evidence for the existence of compounds containing Si=Si double bonds (disilenes) in 1981,[1] there has been a growing interest in the physical and chemical properties of these intriguing compounds.[2] A large number of distinctive reactions of stable disilenes have been reported so far.[3,4] In contrast to C=C double bonds, Si=Si double bonds have been shown to react with a variety of reagents smoothly, and without catalysts, to give corresponding adducts.[5,6] In fact, adduct formation of unsaturated silicon is probably a more widely encountered phenomenon than initially thought. It is the wide variety of reactions known for disilenes that makes them an important building block in organosilicon chemistry. Nevertheless, few thorough investigations into the mechanisms of these reactions have taken place, and mechanistic details are sparse in

* E-mail: midesu@cc.kmu.edu.tw.

(1) West, R.; Fink, M. J.; Michl, J. *Science* **1981**, *214*, 1343.

(2) For reviews on disilenes, see: (a) West, R. *Pure Appl. Chem*. **1984**, *56*, 163. (b) Raabe, G.; Michl, J. *Chem. Rev*. **1985**, *85*, 419. (c) Cowley, A. H.; Norman, N. C. *Prog. Inorg. Chem*. **1986**, *34*, 1 (d) West, R. *Angew. Chem., Int. Ed. Engl*. **1987**, *26*, 1201. (e) Raabe, G.; Michl, J. In *The Chemistry of Organic Silicon Compounds*; Patai, S., Rappoport, Z., Eds.; Wiley: New York, 1989; Part 2, Chapter 17. (f) Tsumuraya, T.; Batcheller, S. A.; Masamune, S. *Angew. Chem., Int. Ed. Engl*. **1991**, *30*, 902. (g) Grev, R. S. *Adv. Organomet. Chem*. **1991**, *33*, 125. (h) Weidenbruch, M. *Coord. Chem. Rev.* **1994**, *130*, 275. (i) Okazaki, R.; West, R. *Adv. Organomet. Chem.* **1996**, *39*, 231. (j) Power, P. P. *J. Chem. Soc., Dalton Trans.* **1998**, 2939. (k) Power, P. P. *Chem. Rev.* **1999**, *99*, 3463. (l) Kira, M.; Iwamoto, T. *J. Organomet. Chem.* **2000**, *610*, 236.

(3) (a) Wiberg, N. *Coord. Chem. Rev.* **1997**, *163*, 217. (b) Wiberg, N.; Niedermayer, W.; Polborn, K.; Noth, H.; Knizek, J.; Fenske, D. Baum, G. In *Organosilicon Chemistry IV*; Auner, N., Weis, J., Eds.; Wiley-VCH: Weinheim, Germany, 2000; p 93. (c) Wiberg, N.; Niedermayer, W.; Polborn, K.; Mayer, P. *Chem.—Eur. J.* **2002**, *8*, 2730 and references therein.

(4) (a) Sekiguchi, A.; Maruki, I.; Sakurai, H. *J. Am. Chem. Soc*. **1993**, *115*, 11460. (b) Sakurai, H. In *The Chemistry of Organic Silicon Compounds*; Rappoport, Z., Apeloig, Y., Eds.; Wiley: New York, 1998; Vol. 2, Part 1, Chapter 15. (c) Apeloig, Y.; Nakash, M. *J. Am. Chem. Soc*. **1996**, *118*, 9798. (d) Apeloig, Y.; Nakash, M. *Organometallics* **1998**, *17*, 1260. (e) Apeloig, Y.; Nakash, M. *Organometallics* **1998**, *17*, 2307. (f) Takahashi, M.; Veszpremi, T.; Hajgato, B.; Kira, M. *Organometallics* **2000**, *19*, 4660.

(5) (a) There is growing evidence from both theory and experiment that the unsaturated disilenes exhibit chemical features that are quite dissimilar from analogous carbon-containing compounds. This is not altogether surprising; indeed, rather simple qualitative arguments indicate that p-type atomic orbitals play a more important role than s orbitals in hybridization in silicon hydrides (see ref 6). This is in contrast to carbon hydrides in which s and p functions are comparably balanced in the formation of sp-, sp^2-, and sp^3-hybrid orbitals. As a result, certain chemical properties, such as equilibrium geometries and reactivity, can exhibit striking features in these compounds. (b) Teramae, H. *J. Am. Chem. Soc.* **1987**, *109*, 4140.

(6) Goddard, W. A.; Harding, L. B., III *Annu. Rev. Phys. Chem*. **1978**, *29*, 363.

10.1021/ic0303340 CCC: $27.50
Published on Web 07/03/2004

Scheme 1

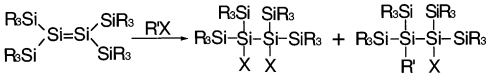

R_3Si = *t*-$BuMe_2Si$, i-Pr_2MeSi, and i-Pr_3Si
R'X = CCl_4, CBr_4, $CHCl_3$, CH_2Cl_2, and CH_3Br

all but a few cases, such as the addition of water, aldehydes, and alcohols to disilenes.[7]

Recently, West et al.[8] and Kira et al.[9] have found that disilenes react very smoothly with various haloalkanes in the dark. These unusual reactions are summarized in Scheme 1. For instance, reactions of tetrasilyldisilene with carbon tetrachloride and carbon tetrabromide at −50 °C in the dark gave the corresponding 2,3-dihalotetrasilane (X = Cl or Br) in high yields.[9] Also, reactions of tetrasilyldisilene with chloroform and dichloromethane readily gave the corresponding 1,2-adducts of the alkyl halides.[9] The formation of these products suggests that the reaction is of a radical nature. Indeed, the involvement of radicals in such reactions has been verified through electron paramagnetic resonance (EPR) studies.[9b] However, little definitive information (such as activation energies and reaction mechanisms) has been obtained about the abstraction reactions due to difficulties in probing these reactions experimentally.[9] The currently accepted mechanism involves forming neutral radical pairs from two closed-shell molecules in the first step.[9] To the best of our knowledge, no similar reactions have been observed between alkenes and haloalkanes. It is therefore important to understand the reaction mechanism to achieve further precise control of the total reaction process.

Furthermore, despite the considerable interest that has been shown in disilenes and their organosilicon chemistry over the past 20 years,[1] the chemistry of heavier group 14 doubly bonded species has not been similarly investigated. Now that compounds containing Ge═Ge, Sn═Sn, and Pb═Pb double bonds can be synthesized and isolated at room temperature,[10] it is natural to consider whether reactions analogous to those shown in Scheme 1 can be extended to these heavier group 14 doubly bonded systems. Neither experimental nor theoretical studies have been carried out on their abstraction reactions with halocarbons, let alone a systematic study of the effect of substitution on the reactivities of the heavier alkene species. Indeed, from being initially a scientific oddity, namely, feasible intermediates in certain chemical reactions, molecular species exhibiting double bonds to heavier group 14 elements have become compounds of definite stability whose specific chemical reactivity is the subject of an increasing number of studies.

We therefore present a density functional theory (DFT) study of the following reactions:

$$(SiH_3)_2X{=}X(SiH_3)_2 + CCl_4 \rightarrow [(SiH_3)_2X{-}X(SiH_3)_2Cl]^\bullet + CCl_3^\bullet \quad (1a)$$

$$(SiH_3)_2X{=}X(SiH_3)_2 + CCl_4 \rightarrow [(SiH_3)_2X{-}X(SiH_3)_2CCl_3]^\bullet + Cl^\bullet \quad (1b)$$

$$X = C, Si, Ge, Sn, Pb$$

$$(SiH_3)_2Si{=}Si(SiH_3)_2 + CY_4 \rightarrow [(SiH_3)_2Si{-}Si(SiH_3)_2Y]^\bullet + CY_3^\bullet \quad (2a)$$

$$(SiH_3)_2Si{=}Si(SiH_3)_2 + CY_4 \rightarrow [(SiH_3)_2Si{-}Si(SiH_3)_2CY_3]^\bullet + Y^\bullet \quad (2b)$$

$$Y = F, Cl, Br, I$$

That is, we consider theoretically the reaction paths of a model abstraction reaction of CY_4 (Y = F, Cl, Br, and I) by a series of tetrasilyldimetallenes of the type $(SiH_3)_2X{=}X(SiH_3)_2$, where X = C, Si, Ge, Sn, and Pb. As can be seen in Scheme 1, two plausible mechanisms are suggested for the reactions of tetrasilyldisilenes with haloalkanes to give the corresponding 1,2-dihalodisilanes and/or 1-alkyl-2-chlorodisilanes.[9] These can be classified into two types on the basis of the order of chemical events in each pathway: (a) the halogen (Y) abstraction; (b) the CY_3 abstraction.[11] Each of these pathways was examined computationally, and each is described in detail below.

Our choice of eqns 1 and 2 as model systems was made for several reasons. First, tetrasilyldimetallenes ($(SiH_3)_2X{=}X(SiH_3)_2$) were chosen as model reactants instead of tetrahydrodimetallenes ($H_2X{=}XH_2$) to mimic the systems for which there are experimental results, namely Scheme 1. Besides this, it was found by ab initio molecular orbital calculations that the diradical character of the former is greater than that of the latter.[5b,9a] We therefore believe that the present models employed in this study will provide reliable information for the discussion of the abstraction mechanism. Second, it has been noted previously that the reactivities of tetrasilyldisilenes toward alkyl halides are qualitatively comparable to those of triethylsilyl radicals.[9a] The rate constant for halogen abstraction by the triethylsilyl radical decreases in the following order: $CCl_4 > CH_3Br > CHCl_3 > CH_2Cl_2$.[12] For this reason, we chose carbon tetrahalides (CY_4) as the model reactants in this study. However, it should be pointed out that our focus on the

(7) (a) Mmorkin, T. L.; Owens, T. R.; Leigh, W. J. In *The Chemistry of Organic Silicon Compounds*; Rappoport, Z., Apeloig, Y., Eds.; John Wiley and Sons: New York, 2001; Vol. 3, p 949. (b) Morkin, T. L.; Leigh, W. J. *Acc. Chem. Res.* **2001**, *34*, 129. (c) Leigh, W. J. *Pure Appl. Chem.* **1999**, *71*, 453. (d) Sakurai, H. In *The Chemistry Organic Silicon Compounds*; Rappoport, Z., Apeloig, Y., Eds.; John Wiley and Sons: New York, 1998; Vol. 2, p 827. (e) Wieberg, N.; Fischer, G.; Schurz, K. *Chem. Ber.* **1987**, *120*, 1605. (f) Mosey, N. J.; Baines, K. M.; Woo, T. K. *J. Am. Chem. Soc.* **2002**, *124*, 13306.

(8) Fanta, A. D.; Belzner, J.; Powell, D. R.; West, R. *Organometallics* **1993**, *12*, 2177.

(9) (a) Iwamoto, T.; Sakurai, H.; Kira, M. *Bull. Chem. Soc. Jpn.* **1998**, *71*, 2741. (b) Kira, M.; Ishima, T.; Iwamoto, T.; Ichinohe, M. *J. Am. Chem. Soc.* **2001**, *123*, 1676.

(10) For the most recent reviews on homonuclear double bonding in heavier group 14 elements, see refs 1j−l.

(11) Kira and co-workers have proposed a third possible mechanism, namely the single-electron transfer (SET) from disilene to haloalkane followed by the coupling of the disilene cation radicals and chloride anion. However, it was also reported by Kira et al. that these disilenes have relatively high oxidation potentials. Therefore, it is unikely that the SET mechanism plays any part in the initial reaction of disilenes with haloalkanes. See ref 9b. For this reason, we exclude the SET mechanism and will not discuss it further in this work.

abstraction of carbon tetrahalides does not imply that the abstraction reactions of other alkyl halides are not important. It means only that we admit to the complexity of the problem and choose to treat the CY_4 abstraction aspects separately. Hence, to reduce the complexity of the problem we chose a simple system ($(SiH_3)_2X{=}X(SiH_3)_2 + CY_4$) in which the determining variable is the efficiency of abstraction reactions. Hydrogen abstraction can be considered later as an effect, which may or may not influence the halogen abstraction. Third, it is reasonable to expect that the variations in group 14 element X and in halogen Y should reveal the electronic influence of both the tetrasilyldimetallenes and the carbon tetrahalides on reactivity. Finally, organic reactions involving halocarbons exhibit considerable mechanistic variety. Equations 1 and 2 should be favorable cases for determining whether more than one mechanism might be operative. We anticipate that the results obtained in this work will allow us to predict the reaction pathway for some known and/or as yet unknown systems. Therefore, detailed investigation into these useful and interesting processes should involve both experimental and theoretical work.

II. Theoretical Methods

All geometries were fully optimized without imposing any symmetry constraints, although in some instances the resulting structure showed various elements of symmetry. For our DFT calculations, we used the hybrid gradient-corrected exchange functional proposed by Becke,[13] combined with the gradient-corrected correlation functional of Lee, Yang, and Parr.[14] This functional is commonly known as B3LYP and has been shown to be quite reliable both for geometries and energies.[15,16] These B3LYP calculations were carried out with relativistic effective core potentials on group 14 elements modeled using the double-ζ (DZ) basis sets[17] augmented by a set of d-type polarization functions.[18] The DZ basis set for the hydrogen element was augmented by a set of p-type polarization functions (p exponents 0.356). The d exponents used for Cl, C, Si, Ge, Sn, and Pb are 0.648, 0.587, 0.296, 0.246, 0.186, and 0.179, respectively. Accordingly, we denote our B3LYP calculations by B3LYP/LANL2DZdp. The spin-unrestricted (UB3LYP) formalism was used for the open-shell (doublet) species. The S^2 expectation values of the doublet state for the radical products all showed an ideal value (0.750) after spin annihilation, so that their geometries and energetics are reliable for this study. Basis set superposition error was not corrected for.[19] Frequency calculations were performed on all structures to confirm that the reactants, intermediates, and products had no imaginary frequencies and that transition states possessed only one imaginary frequency. The relative energies were thus corrected for vibrational zero-point energies (ZPE, not scaled). All of the DFT calculations were performed using the GAUSSIAN 98 package of programs.[20]

III. Results and Discussion

1. Geometries and Energetics of $(SiH_3)_2X{=}X(SiH_3)_2$. Before discussing the geometrical optimizations and the potential energy surfaces for the abstraction reactions, we shall first review the geometries and energies of the silyl-substituted dimetallene reactants, i.e., $(SiH_3)_2X{=}X(SiH_3)_2$.

(12) (a) Chatgilialoglu, C.; Ingold, K. U.; Scaiano, J. C. *J. Am. Chem. Soc.* **1982**, *104*, 5123. (b) Chatgilialoglu, C. *Chem. Rev.* **1995**, *95*, 1229 and references therein.

(13) (a) Becke, A. D. *Phys. Rev. A* **1988**, *38*, 3098. (b) Becke, A. D. *J. Chem. Phys*. **1993**, *98*, 5648.

(14) Lee, C.; Yang, W.; Parr, R. G. *Phys. Rev. B* **1988**, *37*, 785.

(15) (a) Jursic, B. *Chem. Phys. Lett.* **1996**, *256*, 603. (b) Jursic, B. *J. Mol. Struct. (THEOCHEM)* **1998**, *425*, 145. (c) Niu, S.; Hall, M. B. *Chem. Rev*. **2000**, *100*, 353. (d) Bartlett, K. L.; Goldberg, K. I.; Borden, W. T. *J Am. Chem. Soc.* **2000**, *122*, 1456. (e) Irigoeas, A.: Mercero, J. M.; Silanes, I.; Ugalde, J. M. *J. Am. Chem. Soc*. **2001**, *123*, 5040.

(16) It has been shown previously that in critical cases the B3LYP method severely underestimates the stability of dimers relative to their silylene precursors [Takahashi, M.; Tsutsui, S.; Sakamoto, K.; Kira, M.; Muller, T.; Apeloig, Y. *J. Am. Chem. Soc*. **2001**, *123*, 347]. Nevertheless, it has also been reported in a recent paper that the B3LYP-optimized geometries were found to be an accurate representation of the diradical structures, especially for some addition reactions of (di)metallenes (see ref 7f). Accordingly, to validate our choice of method, we performed test calculations using the CCSD method. CCSD/LANL2DZdp single-point energy calculations were performed on the B3LYP/LANL2DZdp geometries of $(SiH_3)_2Si{=}Si(SiH_3)_2$, CCl_4, and transition structures, i.e., $(SiH_3)_2Si{=}Si(SiH_3)_2 + CCl_4 \rightarrow$ Cl-abstraction-TS and $(SiH_3)_2Si{=}Si(SiH_3)_2 + CCl_4 \rightarrow CCl_3$-abstraction-TS. Our computational results showed that these activation barriers calculated at the CCSD/LANL2DZdp//B3LYP/LANL2DZdp level (8.7 and 65 kcal/mol) are not significantly different from those computed at the B3LYP/LANL2DZdp level (10 and 61 kcal/mol). Using identical hardware and software, each CCSD/LANL2DZdp single-point calculation took an average of >165 times longer to complete than a B3LYP/LANL2DZdp single-point calculation on the same geometry. Since the qualitative features of the potential energy profiles of the B3LYP and CCSD levels are similar to each other, the use of the former is sufficient to provide qualitatively correct results. Moreover, it should be pointed out that comparative studies are very useful in understanding similarities and differences in the chemical properties of compounds. In such cases, trends in the properties of interest can often be more important than their absolute values. While making such comparisons, the properties can be studied as a function of substituents, or periodic trends can be examined by studying the properties of compounds with elements from the same period or group. These options provide a criterion for testing the consistency of a given level of calculation. In addition, this method also allows properties to be predicted for compounds that are not yet amenable to experiment.

(17) (a) Dunning, T. H., Jr.; Hay, P. J. In *Modern Theoretical Chemistry*; Schaefer, H. F., III, Ed.; Plenum: New York, 1976; pp 1−28. (b) Hay, P. J.; Wadt, W. R. *J. Chem. Phys*. **1985**, *82*, 270. (c) Hay, P. J.; Wadt, W. R. *J. Chem. Phys*. **1985**, *82*, 284. (d) Hay, P. J.; Wadt, W. R. *J. Chem. Phys*. **1985**, *82*, 299.

(18) Check, C. E.; Faust, T. O.; Bailey, J. M.; Wright, B. J.; Gilbert, T. M.; Sunderlin, L. S. *J. Phys. Chem. A* **2001**, *105*, 8111.

(19) Basis set superposition errors (BSSEs) were not taken into account in the present work for two reasons: (1) A number of previous works on the reactivity of radical addition to alkenes conclude that the values of BSSEs do not converge within the size of the basis sets employed, and what is still worse, corrections to the barrier heights values using calculated BSSEs drastically reduce any agreement with experiments (see for example: (a) Pudzianowski, A. T. *J. Chem. Phys.* **1995**, *102*, 8029. (b) Sule, P.; Nagy, A. *J. Chem. Phys.* **1996**, *104*, 8524. (c) Liedl, K. R. *J. Chem. Phys.* **1998**, *108*, 3199. (d) Samanta, U.; Chakrabarti, P.; Chandrasekhar, J. *J. Phys. Chem. A* **1998**, *102*, 8694. (e) Everaert, G. P.; Herrebout, W. A.; van der Veken, B. J.; Lundell, J.; Rasaneu, M. *Chem.−Eur. J.* **1998**, *4*, 321). (2) The BSSEs do not affect the calculation of barrier heights in the case of processes involving intermediate complexes such as the ones in this work (see for example: Sordo, J. A. *J. Chem. Phys.* **1997**, *106*, 6204). In any case, it is not expected that a BSSE correction would convert them into unstable structures.

(20) Frisch, M. J.; Trucks, G. W.; Schlegel, H. B.; Scuseria, G. E.; Robb, M. A.; Cheeseman, J. R.; Zakrzewski, V. G.; Montgomery, J. A., Jr.; Stratmann, R. E.; Burant, J. C.; Dapprich, S.; Millam, J. M.; Daniels, A. D.; Kudin, K. N.; Strain, M. C.; Farkas, O.; Tomasi, J.; Barone, V.; Cossi, M.; Cammi, R.; Mennucci, B.; Pomelli, C.; Adamo, C.; Clifford, S.; Ochterski, J.; Petersson, G. A.; Ayala, P. Y.; Cui, Q.; Morokuma, K.; Malick, D. K.; Rabuck, A. D.; Raghavachari, K.; Foresman, J. B.; Cioslowski, J.; Ortiz, J. V.; Baboul, A. G.; Stefanov, B. B.; Liu, Liashenko, G.; Piskorz, A.; Komaromi, P.; I.; Gomperts, R.; Martin, R. L.; Fox, D. J.; Keith, T.; Al-Laham, M. A.; Peng, C. Y.; Nanayakkara, A.; Gonzalez, C.; Challacombe, M.; Gill, P. M. W.; Johnson, B.; Chen, W.; Wong, M. W.; Andres, J. L.; Gonzalez, C.; Head-Gordon, M.; Replogle, E. S.; Pople, J. A. *GAUSSIAN 98*; Gaussian, Inc.: Pittsburgh, PA, 1998.

Table 1. Selected Geometric Values and Relative Energies for Singlet and Triplet Dimetallenes, $(SiH_3)_2X{=}X(SiH_3)_2$, Where X = C, Si, Ge, Sn, and Pb[a]

system (X=X)	geometry (singlet)	X=X(singlet) (Å)	θ[b] (deg)	B3LYP[c] (kcal/mol)	X=X(triplet) (Å)	ΔE_{st}[d] kcal mol^{-1})
C=C	plane	1.373	0.0	0.0	1.454	+36.23
Si=Si	plane	2.148	0.0	0.0	2.301	+21.29
Ge=Ge	plane	2.283	0.0	+0.4067	2.480	+17.19
	trans-bent	2.307	27.1	0.0		
Sn=Sn	plane	2.608	0.0	+3.651	2.861	+12.48
	trans-bent	2.706	42.9	0.0		
Pb=Pb	plane	2.671	0.0	+14.18	2.997	+10.69
	trans-bent	2.884	47.6	0.0		

[a] All were calculated at the B3LYP/LANL2DZdp level of theory. [b] The pyramidalization angle θ is defined in **1**. [c] Energies relative to trans-bent geometries. [d] Energy relative to the corresponding singlet state. A positive value means the singlet is the ground state.

The electronic structures and geometries of dimetallenes have been extensively studied by many groups.[21] It is well-known that the heavier analogues of olefins ($R_2X{=}XR_2$) do not exhibit classical planar geometry but rather have a trans-bent structure (**1**), with pyramidalization of both XR_2 groups.[21] Indeed, these compounds, containing so-called "nonclassical double bonds", have been proved to be the preferred arrangements for disilene and digermene and are local minima on the potential energy surface for all of the heavier analogues of ethylene, from Si_2H_4 to Pb_2H_4.[22] Interested readers can find excellent reviews in ref 21.

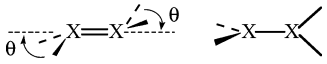

1 **2**

In this work, geometry optimizations were performed on the silyl-substituted dimetallene, $(SiH_3)_2X{=}X(SiH_3)_2$, in an attempt to obtain both singlet planar and trans-bent structures as well as the first triplet structures to allow for the subsequent comparison of the stabilities of these three geometries. Selected geometric values of the singlet planar, singlet trans-bent, and the first triplet dimetallenes, as well as the energies relative to the trans-bent reactants, are given in Table 1. Our computational results suggest that only planar structures are stable for silyl-substituted ethylene and disilene,[23] whereas stationary points corresponding to both planar and trans-bent structures were located for silyl-substituted digermene, distannene, and diplumbene on the B3LYP potential energy surfaces. The energies show that the planar structure becomes less stable with respect to the trans-bent one as heavier atoms become involved in the double bond. The magnitude of the pyramidalization angle θ (see **1**) also increases with this change. Apparently, the heavier main group elements are pivotal atoms in this regard. These results are consistent with those reported in the previous studies cited above and will not be discussed further.

On the other hand, the relative energies and selected geometric values based on B3LYP calculations for the first triplet dimetallenes are also reported in Table 1. To the best of our knowledge, neither experimental nor theoretical work on the triplet substituted dimetallenes has been reported so far. Molecular orbital (MO) theory[24] predicts that the triplet state of dimetallene adopts the perpendicular structure as shown in **2**. Our DFT results confirm this prediction. An interesting trend that can be observed in Table 1 is the increase in the X−X bond distance on going from the singlet to the triplet state. The reason for this phenomenon can be understood simply by considering the electronic structures of the two states.[24] Moreover, as seen in Table 1, our DFT calculations indicate that the singlet−triplet energy splitting of dimetallenes generally decreases as the atomic number of the central atom is increased. That is to say, the stability of the singlet state decreases with decreasing electronegativity at the central atoms X=X. Again, the reason for this can be derived from basic MO theory.[24] Namely, distortion from planar to trans-bent in a 12-valence-electron dimetallene system results in a decrease in the HOMO and LUMO energy gap due to the second-order Jahn−Teller effect (vide infra). See **3**. This, in turn, leads to a decrease in the singlet−triplet energy splitting of dimetallene on going down a column in the periodic table. We shall use the above results to explain the origin of barrier heights for the abstraction reactions in a later section.

2. Geometries and Energetics of $(SiH_3)_2X{=}X(SiH_3)_2$ + CCl_4. Next, let us consider radical mechanisms which proceed via eq 1, focusing on the transition states as well as

(21) For instance, see: (a) Liang, C.; Allen, C. C. *J. Am. Chem. Soc.* **1990**, *112*, 1039. (b) Karni, M.; Apeloig, Y. *J. Am. Chem. Soc.* **1990**, *112*, 8589. (c) Grev, R. S. *Adv. Organomet. Chem.* **1991**, *33*, 125. (d) Okazaki, R.; West, R. *Adv. Organomet. Chem.* **1996**, *39*, 31. (e) Power, P. P. *J. Chem. Soc., Dalton Trans.* **1998**, 2939. (f) Barrau, J.; Rima, G. *Coord. Chem. Rev.* **1998**, *178*, 593. (g) Escudié, J.; Couret, C.; Ranaivonjatovo, H. *Coord. Chem. Rev.* **1998**, *178*, 565. (h) Leigh, W. *J. Pure. Appl. Chem.* **1999**, *71*, 453. (i) Robinson, G. H. *Acc. Chem. Res.* **1999**, *32*, 773. (j) Power, P. P. *Chem. Rev.* **1999**, *99*, 3463. (k) Leigh, W. J. *Pure Appl. Chem.* **1999**, *71*, 453.

(22) (a) Trinquier, G. *J. Am. Chem. Soc.* **1990**, *112*, 2130. (b) Trinquier, G. *J. Am. Chem. Soc.* **1991**, *113*, 144. (c) Jacobsen, H.; Ziegler, T. *J. Am. Chem. Soc.* **1994**, *116*, 3667. (d) Kapp, J.; Remko, M.; Schleyer, P. v. R. *Inorg. Chem.* **1997**, *36*, 241.

(23) According to a model suggested independently by Carter and Goddard and by Trinquier and Malrieux (the CGMT model; for recent review, see: Driess, M.; Grutzmacher, H. *Angew. Chem., Int. Ed. Engl.* **1996**, *35*, 828), the tendency of doubly bonded molecules (such as $R_2X{=}XR_2$) to distort from the planar should depend on the magnitude of singlet−triplet energy gap ($\Delta E_{st} = E_{triplet} - E_{singlet}$) of the corresponding divalent species, R_2X:. As a result, our B3LYP/LANL2DZdp calculations estimate that the ΔE_{st} of $(SiH_3)_2X$: are −22.3, +2.19, +12.5, +16.7, and +24.5 kcal/mol for X = C, Si, Ge, Ge, Sn, and Pb. From these data, it therefore not surprising that both $(SiH_3)_2C{=}C(SiH_3)_2$ and $(SiH_3)_2Si{=}Si(SiH_3)_2$ adopt a planar geometry, whereas other tetrasilyldimetallenes take the trans-bent structures. For more details, also see: Chen, W.-C.; Su, M.-D.; Chu, S.-Y. *Organometallics* **2001**, *20*, 564.

(24) Albright, T. A.; Burdett, J. K.; Whangbo, M.-H. *Orbital Interactions in Chemistry*; John Wiley & Sons: New York, 1985; p 164.

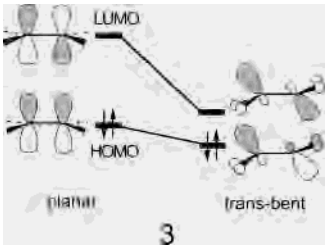

3

on the abstraction products themselves. If one starts from the stable precursor complex, the reaction of $(SiH_3)_2X{=}X(SiH_3)_2$ with CCl_4 can take place from two directions: the abstraction of a chlorine atom from CCl_4 to produce $[X{=}X]{-}Cl^{\bullet}$ and $CCl_3^{\bullet}$ products (shown in eq 1a) or the $CCl_3^{\bullet}$ radical transfer to [X═X] leading to the formation of $[X{=}X]{-}CCl_3^{\bullet}$ and $Cl^{\bullet}$ products (shown in eq 1b). Here [X═X] stands for $(SiH_3)_2X{=}X(SiH_3)_2$. Briefly, such radical mechanisms may be thought to proceed as follows: reactants (**Rea**) → precursor complex (**Pcx**) → transition state (**TS**) → radical products (**Pro**). Information about the transition states of the $(SiH_3)_2X{=}X(SiH_3)_2$ radical abstraction reaction is one of the most interesting results of this study since very little is known about the barrier heights.

The optimized geometries calculated at the B3LYP/LANL2DZdp level of theory involving reactants, precursor complex, transition state, and products of the two kinds of reaction mechanisms (i.e., eq 1a,b) are collected in Figures1−5 for $(SiH_3)_2X{=}X(SiH_3)_2$, where X = C, Si, Ge, Sn, and Pb, respectively. For convenience, we have also given the energies relative to the two reactant molecules, i.e., $(SiH_3)_2X{=}X(SiH_3)_2 + CCl_4$. Moreover, to simplify comparisons, and to emphasize the trends, the calculated heats of reaction and the individual barrier heights are also summarized in Table 2. The major conclusions that can be drawn from Figures 1−5 and Table 2 are as follows.

(1) Considering the Cl-abstraction reaction path, we have located the transition state for each $(SiH_3)_2X{=}X(SiH_3)_2$ case (**TS-1a-C**, **TS-1a-Si**, **TS-1a-Ge**, **TS-1a-Sn**, and **TS-1a-Pb**) at the B3LYP/LANL2DZdp level of theory. The optimized geometries of the five transition states can be found in Figures 1−5, respectively, along with the imaginary frequency eigenvector. One can observe that the main components of the transition vector correspond to the motion of the chlorine atom between the X and the carbon atoms. The eigenvalues give an imaginary frequency (cm^{-1}) of 78.8i (**TS-1a-C**), 106i (**TS-1a-Si**), 94.1i (**TS-1a-Ge**), 85.7i (**TS-1a-Sn**), and 98.2i (**TS-1a-Pb**). As seen in Figures 1−5, the three atoms (X, Cl, and C) involved in the bond-breaking and bond-forming process are not collinear along the X−C axis. This abstracted chlorine atom makes an angle, with respect to the X−C bond, of 140, 152, 152, 153, and 154° for X = C, Si, Ge, Sn, and Pb systems, respectively. Interestingly, the approach of the CCl_4 along the X−C axis is more bent in the ethylene case than in the disilene, digermene, distannene, and diplumbene cases. The breaking Cl−C bond length is generally increased, while the forming X−Cl bond length becomes smaller. For instance, the breaking Cl−C bond lengths are 3.643 Å (C), 2.292 Å (Si), 2.271 Å (Ge), 2.279 Å (Sn), and 2.302 Å (Pb), respectively, whereas the forming X−Cl bond lengths are 0.104 Å (C), 0.224 Å (Si), 0.221 Å (Ge), 0.174 Å (Sn), and 0.198 Å (Pb) longer than that in the $[(SiH_3)_2X{=}X(SiH_3)_2Cl]^{\bullet}$ abstraction product. These values suggest that the delocalization of the unpaired electron take place later along the reaction coordinate. Thus, the X−Cl and Cl−C bond lengths in the transition structure are more reactant-like for X = Sn and Pb and more product-like for X = C. According to the Hammond postulate,[25] **TS-1a-Sn** and **TS-1a-Pb** should have the smallest and **TS-1a-C** the highest activation barriers. This was fully confirmed by our theoretical calculations. As shown in Table 2, the barrier height for the Cl-abstraction reaction decreases in the order (kcal/mol) **TS-1a−C** (+66) > **TS-1a-Si** (+10) > **TS-1a-Ge** (+8.2) > **TS-1a-Sn** (+5.4) > **TS-1a-Pb** (+4.7). In other words, the greater the atomic number of the [X═X] center, the lower the Cl-abstraction barrier.

(2) Next, let us consider the CCl_3-abstraction reaction mechanism. As can be seen in Figures 1−5, the transition state vectors, represented by the heavy arrows in the saddle points (**TS-1b-C**, **TS-1b-Si**, **TS-1b-Ge**, **TS-1b-Sn**, and **TS-1b-Pb**) are all in accordance with the CCl_3-abstraction process, that is with the $Cl{-}CCl_3$ bond stretching and the CCl_3 group migrating toward the X center. From Table 2, it is obvious that the barrier height for CCl_3 abstraction is much higher than that for Cl abstraction for each [X═X] case. For instance, the DFT calculations estimate that the activation energies for Cl- and CCl_3-abstraction reaction paths are (kcal/mol) **TS-1b-C** (+70) > **TS-1a-C** (+66), **TS-1b-Si** (+61) > **TS-1a-Si** (+10), **TS-1b-Ge** (+57) > **TS-1a-Ge** (+8.2), **TS-1b-Sn** (+54) > **TS-1a-Sn** (+5.4), and **TS-1b-Pb** (+56) > **TS-1a-Pb** (+4.7). These results clearly indicate that for each $(SiH_3)_2X{=}X(SiH_3)_2$ system the Cl-abstraction path is much more favorable than the CCl_3-abstraction path under the same reaction conditions. Besides this, it is also found that the energies of the CCl_3-abstraction products, $[(SiH_3)_2X{=}X(SiH_3)_2CCl_3]^{\bullet}$ (X = C, Si, Ge, Sn, and Pb), are above those of the corresponding reactants by 52, 20, 22, 23, and 24 kcal/mol, respectively. On the other hand, the reaction enthalpy of the Cl-abstraction product, $[(SiH_3)_2X{=}X(SiH_3)_2Cl]^{\bullet}$, are calculated to be 36, −11, −9.5, −13, and −13 kcal/mol with respect to their corresponding reactants. Again, these computational results strongly suggest that experimental detection of the CCl_3-abstraction product formed during the reaction is highly unlikely.

In short, the periodic trends in the energetics of the $(SiH_3)_2X{=}X(SiH_3)_2 + CCl_4$ reactions are especially interesting. First, our theoretical findings indicate that for haloalkane abstraction reactions there is a very clear trend toward lower activation barriers and more exothermic interactions on going from carbon to lead along a column. Second, for a given dimetallene, the overall Cl-abstraction reaction is more exothermic and the barrier height lower than for the corresponding CCl_3 abstraction.

3. Geometries and Energetics of $(SiH_3)_2Si{=}Si(SiH_3)_2 + CY_4$. We now consider the abstraction reactions of disilene

(25) Hammond, G. S. *J. Am. Chem. Soc*. **1954**, *77*, 334.

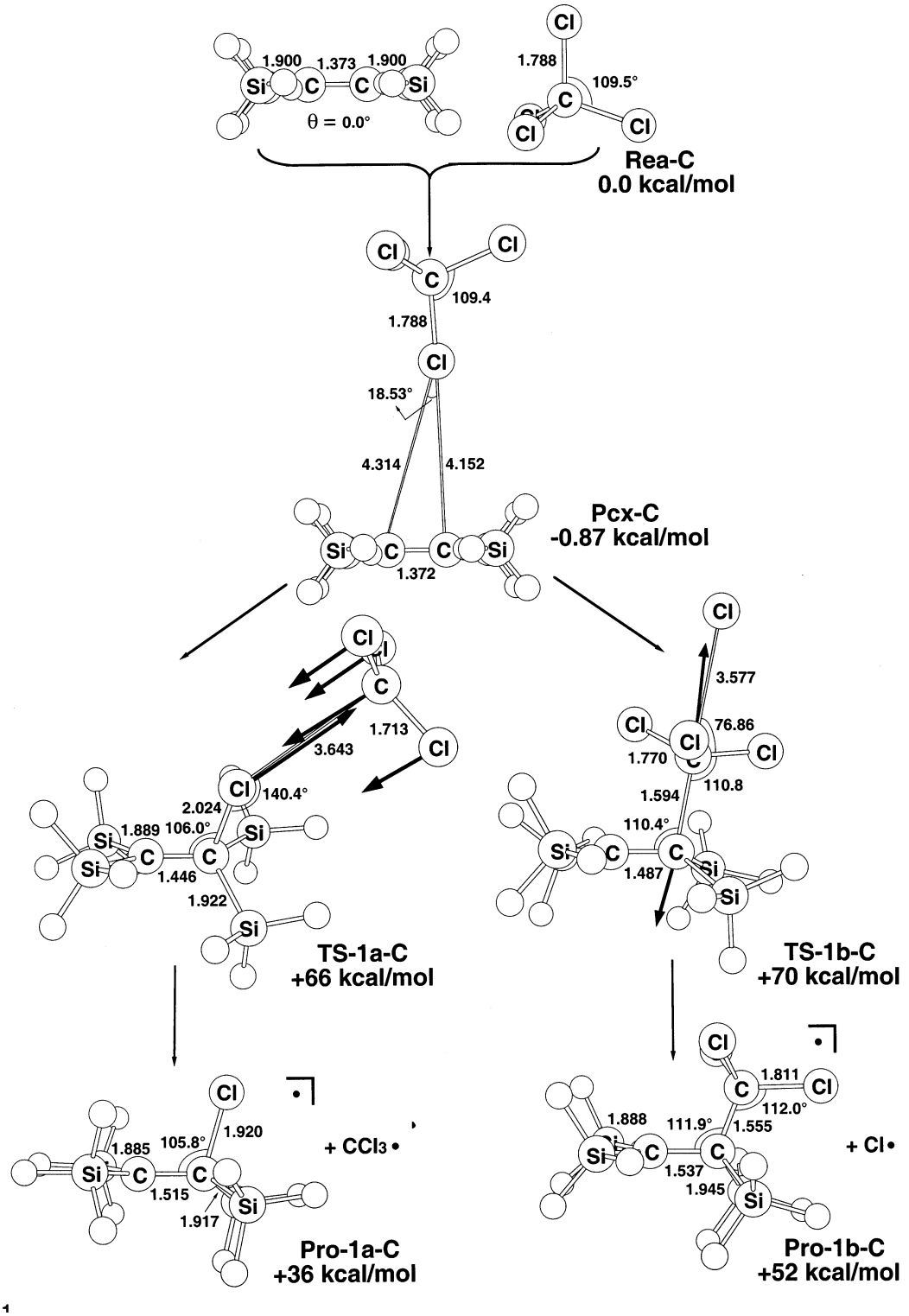

Figure 1. Optimized geometries (in Å and deg) for the reactants (**Rea**), precursor complexes (**Pcx**), transition states (**TSs**), and abstraction products (**Pro**) of $(SiH_3)_2C{=}C(SiH_3)_2$ with CCl_4 through two reaction pathways (1a) and (1b). All were calculated at the B3LYP/LANL2DZdp level of theory. The heavy arrows indicate the main components of the transition vector. Hydrogens are omitted for clarity.

(i.e., $(SiH_3)_2Si{=}Si(SiH_3)_2$) with various carbon tetrahalides (CY_4). Once again, if we start from the precursor complex, the abstraction reaction of $(SiH_3)_2Si{=}Si(SiH_3)_2$ with CY_4 can occur via two reaction pathways: the Y-abstraction reaction path (eq 2a); the CY_3-abstraction reaction path (eq 2b). The results from our theoretical study are summarized in Figures 2, 6, 7, and 8 for Y = Cl, F, Br, and I, respectively. The relative energies of some critical points along the abstraction reaction process, reactants (**Rea**) → precursor complex (**Pcx**) → transition state (**TS**) → products (**Pro**), are collected in Table 3. There are several important and noteworthy conclusions.

(1) Considering the Y-abstraction reaction mechanism, a search for the transition state did show that the energy profile

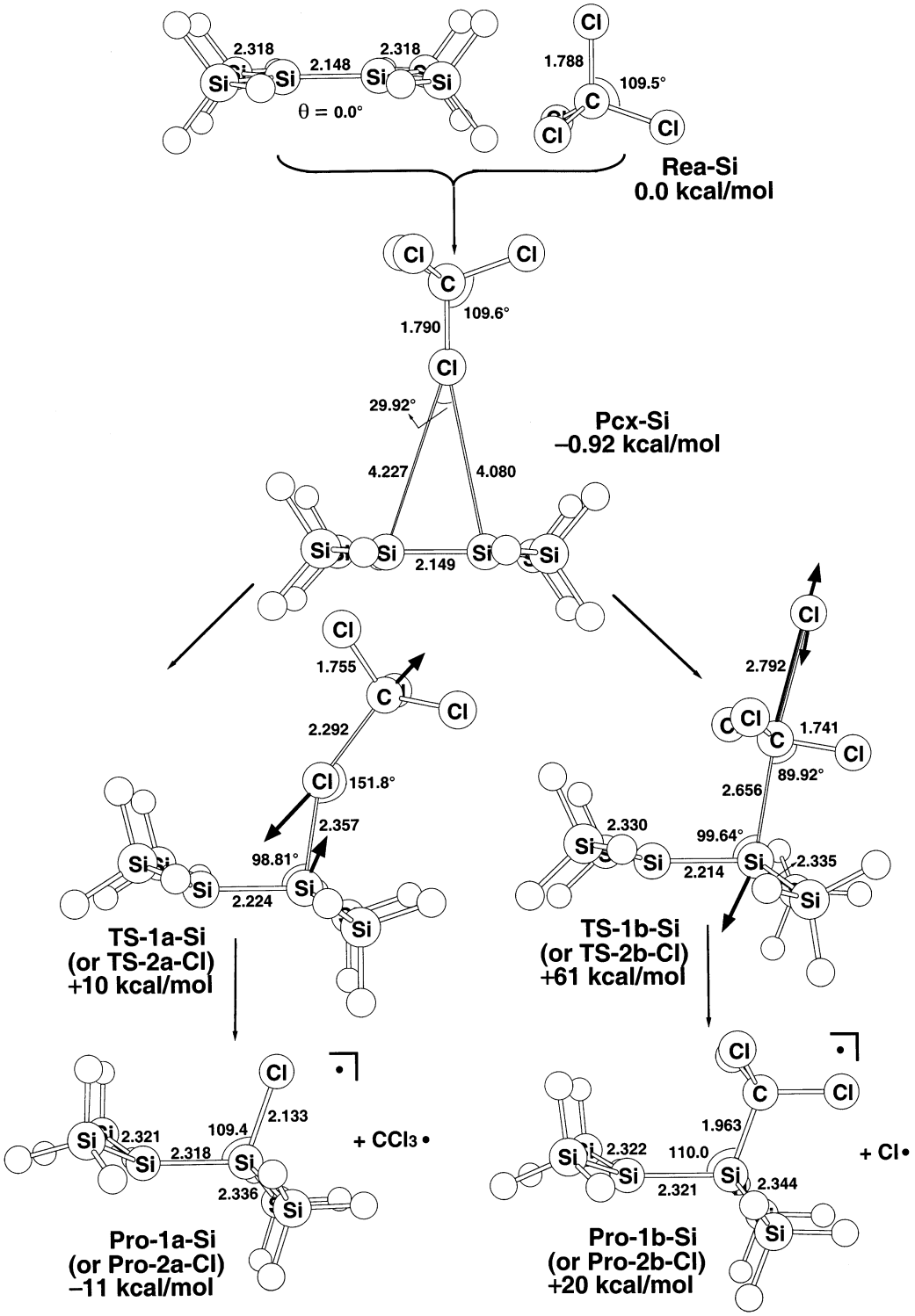

Figure 2. Optimized geometries (in Å and deg) for the reactants (**Rea**), precursor complexes (**Pcx**), transition states (**TSs**), and abstraction products (**Pro**) of $(SiH_3)_2Si{=}Si(SiH_3)_2$ with CCl_4 through two reaction pathways (1a) and (1b). All were calculated at the B3LYP/LANL2DZdp level of theory. The heavy arrows indicate the main components of the transition vector. Hydrogens are omitted for clarity.

for this reaction exhibits a maximum. The transition states located for the Y (Y = F, Cl, Br, and I) abstractions are presented in Figures 6, 2, 7, and 8, respectively. Those transition structures are characterized by one imaginary frequency of 95.4i, 106i, 87.3i, and 88.6i cm^{-1} for **TS-2a-F**, **TS-2a-Cl**, **TS-2a-Br**, and **TS-2a-I**, respectively. The normal coordinate corresponding to the imaginary frequency is primarily the motion of the halogen atom Y separating from the carbon atom of CY_3. Further, as was the case for the various dimetallene abstractions discussed earlier, the carbon of the leaving group CY_3 does not lie on the Si−Y axis in all the carbon tetrahalide cases. One of the interesting points to emerge from calculations of TS geometries is the extent to which the Si−Y bond is formed in the transition

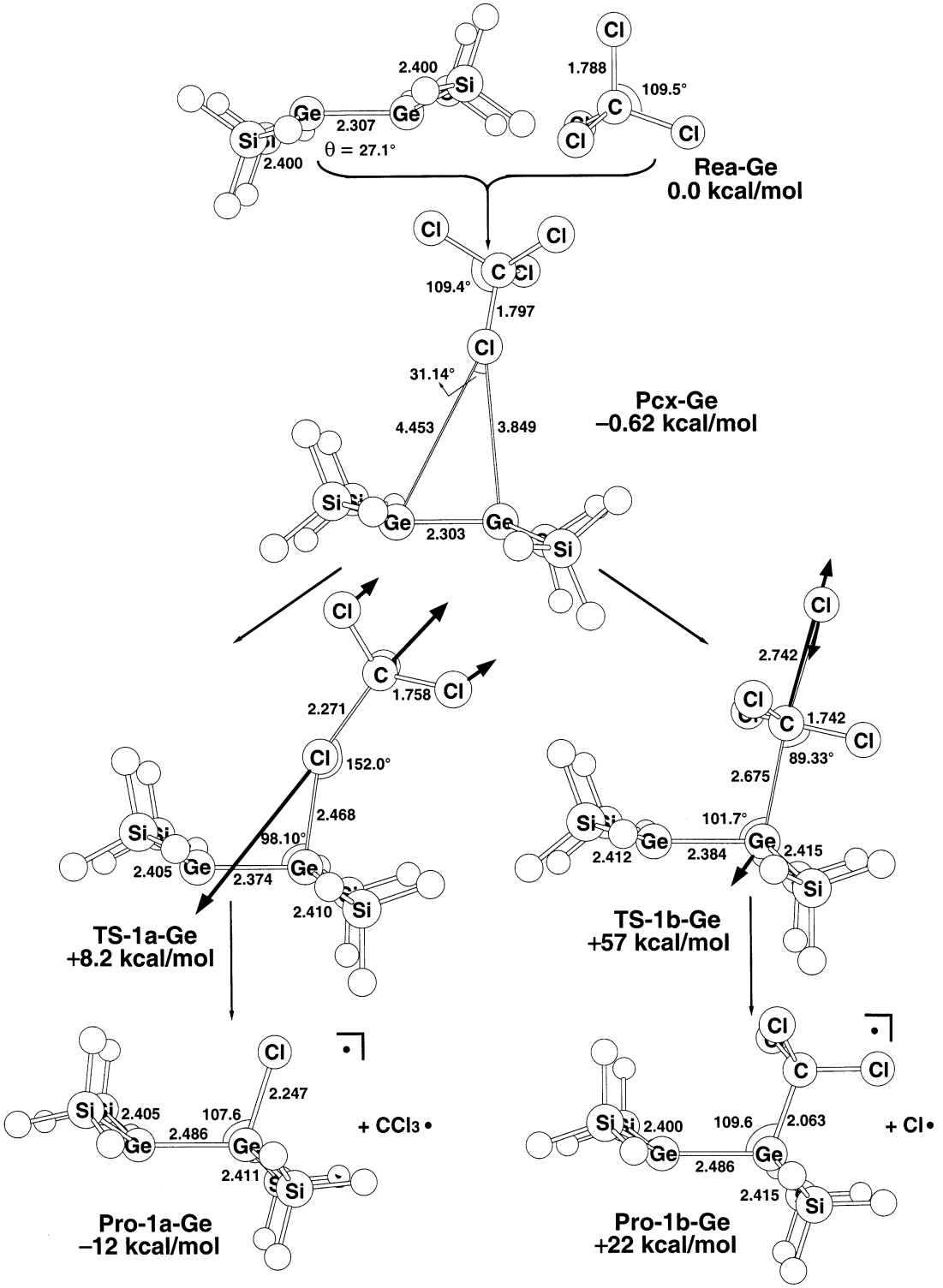

Figure 3. Optimized geometries (in Å and deg) for the reactants (**Rea**), precursor complexes (**Pcx**), transition states (**TSs**), and abstraction products (**Pro**) of $(SiH_3)_2Ge{=}Ge(SiH_3)_2$ with CCl_4 through two reaction pathways (1a) and (1b). All were calculated at the B3LYP/LANL2DZdp level of theory. The heavy arrows indicate the main components of the transition vector. Hydrogens are omitted for clarity.

state. The Si−Y bond lengths in **TS-2a-F**, **TS-2a-Cl**, **TS-2a-Br**, and **TS-2a-I** are 6.0%, 11%, 13%, and 23% longer than those in the corresponding products ($[(SiH_3)_2Si{=}Si(SiH_3)_2Y]^{\bullet}$), respectively. All these features suggest that the Br- and I-abstraction reactions arrive at the TS relatively early, whereas the F-abstraction reaction reaches the TS relatively late. In other words, on the basis of Hammond's postulate, this indicates that the heavier the Y atom, the earlier the transition state is formed. This is also in consistent with the greater exothermicity of the $(SiH_3)_2Si{=}Si(SiH_3)_2 + CY_4$ (Y = Br and I) reaction when compared to that of the $(SiH_3)_2Si{=}Si(SiH_3)_2 + CF_4$ reaction. For instance, as demonstrated in Table 3, the barrier height for the Y-abstraction mechanism decreases in the order (kcal/mol) **TS-2a-F** (+43) > **TS-2a-Cl** (+10) > **TS-2a-Br** (+0.19) > **TS-2a−I** (−4.1). It should be noted that there is no barrier to

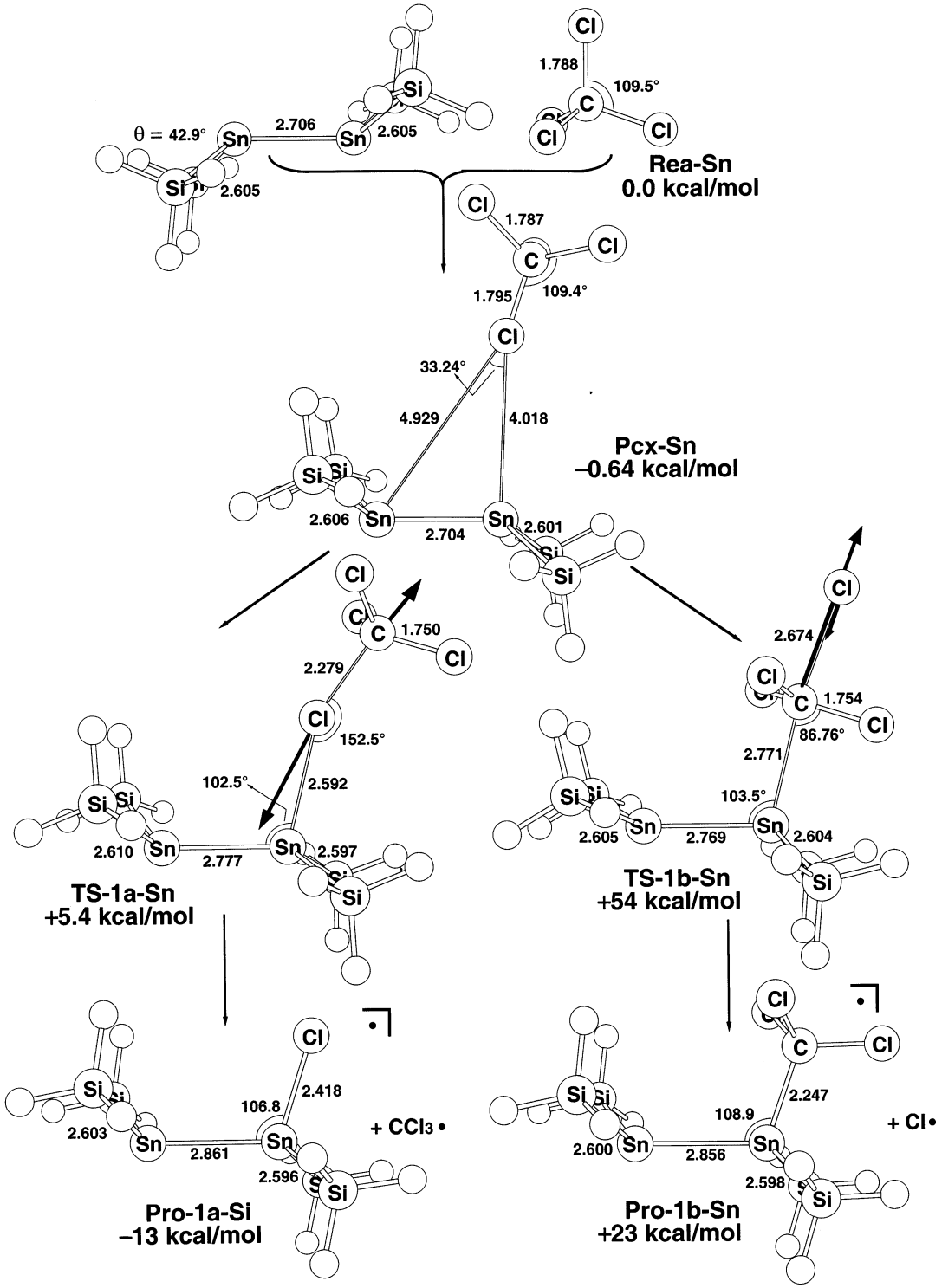

Figure 4. Optimized geometries (in Å and deg) for the reactants (**Rea**), precursor complexes (**Pcx**), transition states (**TSs**), and abstraction products (**Pro**) of $(SiH_3)_2Sn{=}Sn(SiH_3)_2$ with CCl_4 through two reaction pathways (1a) and (1b). All were calculated at the B3LYP/LANL2DZdp level of theory. The heavy arrows indicate the main components of the transition vector. Hydrogens are omitted for clarity.

the iodine abstraction by disilene. Moreover, the order of exothermicity follows the same trend as that of the activation energy (kcal/mol): **Pro-2a-F** (+16) > **Pro-2a-Cl** (−11) > **Pro-2a-Br** (−13) > **Pro-2a−I** (−14). Our model calculations are consistent with some experimental findings.[8,9]

(2) Finally, we consider the CY_3-abstraction reaction mechanism. All the CY_3-abstraction transition states located at the B3LYP level of theory were confirmed by calculation of the energy Hessian which shows only one imaginary vibrational frequency: 714i cm^{-1} (**TS-2b-F**), 534i cm^{-1} (**TS-2b-Cl**), 498i cm^{-1} (**TS-2b-Br**), and 606i cm^{-1} (**TS-2b-I**). Decomposition of the imaginary mode into internal coordinate displacements shows the major component to be the Y_3C-Y bond breaking, as one would expect for a true CY_3-

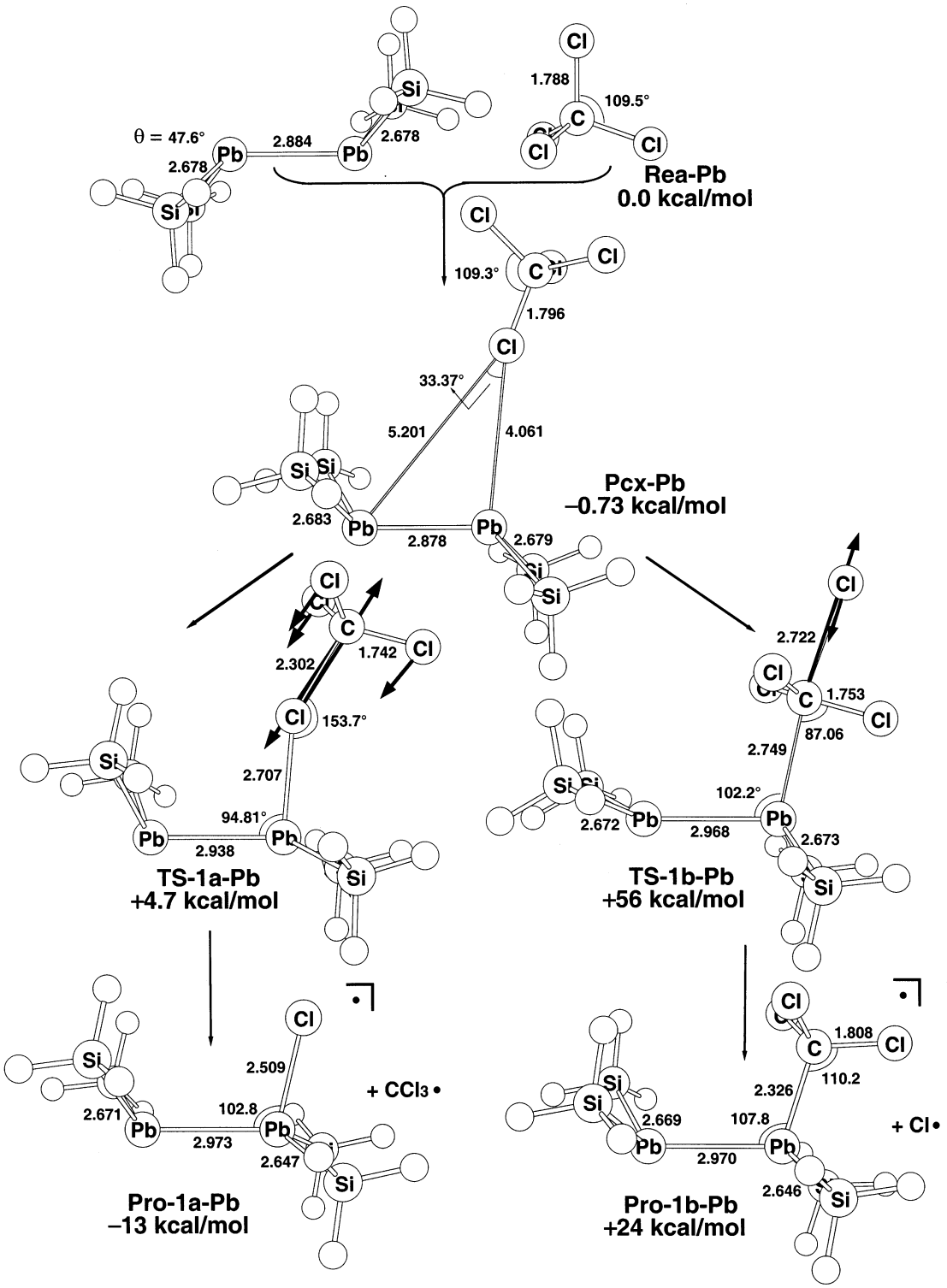

Figure 5. Optimized geometries (in Å and deg) for the reactants (**Rea**), precursor complexes (**Pcx**), transition states (**TSs**), and abstraction products (**Pro**) of $(SiH_3)_2Pb{=}Pb(SiH_3)_2$ with CCl_4 through two reaction pathways (1a) and (1b). All were calculated at the B3LYP/LANL2DZdp level of theory. The heavy arrows indicate the main components of the transition vector. Hydrogens are omitted for clarity.

abstraction TS (see Figures 2 and 6−8). Furthermore, it was found that, in this transition structure, the CF_3 moiety has a strongly pyramidal carbon center, while the CBr_3 and CI_3 moieties have a nearly planar coordination around carbon. Namely, pyramidalization at the CY_3 moiety decreases rapidly from F down to I. The reason for this can be easily understood using simple molecular orbital theory.[26] One intriguing result to emerge from this study is that, for a given carbon tetrahalide, the activation barrier for CY_3 abstraction is considerably larger than that for Y abstraction. For example, as shown in Table 3, the B3LYP results demonstrate that the barrier heights for both Y- and CY_3-abstraction reaction paths are (kcal/mol) **TS-2b-F** (+96) > **TS-2a-F** (+43), **TS-2b-Cl** (+61) > **TS-2a-Cl** (+10), **TS-2b-Br** (+51)

(26) Gimarc, B. M. *Molecular Structure and Bonding*; Academic Press: New York, 1979; p 169.

Table 2. Energies (in kcal/mol) of Stationary Points Relative to the Reactants ($CCl_4 + (SiH_3)_2X{=}X(SiH_3)_2$, Where X = C, Si, Ge, Sn, and Pb)[a]

system[b]	X = C	X = Si	X = Ge	X = Sn	X = Pb
		Reactants			
$CCl_4 + (SiH_3)_2X{=}X(SiH_3)_2$	0.0	0.0	0.0	0.0	0.0
		Precursor Complex			
	−0.872[c]	−0.920[d]	−0.624[e]	−0.638[f]	−0.727[g]
		Cl Abstraction (Path a)			
transition state	+65.5[h]	+9.96[i]	+8.16[j]	+5.41[k]	+4.69[l]
$[X{-}XCl]^{\bullet} + CCl_3^{\bullet}$ [m]	+35.6[n]	−10.7[o]	−11.5[p]	−13.0[q]	−12.5[r]
		CCl_3 Abstraction (Path b)			
transition state	+69.5[s]	+60.7[t]	+56.8[u]	+54.3[v]	+55.8[w]
$[X{-}X\ CCl_3]^{\bullet} + Cl^{\bullet}$ [m]	+51.6[x]	+19.9[y]	+22.0[z]	+22.5[aa]	+23.6[bb]

[a] All at the B3LYP/LANL2DZdp (singlet) or UB3LYP/LANL2DZdp (doublet) levels of theory; see the text. [b] See Figures 1−5 for structures. [c] **Pcx-C**. [d] **Pcx-Si**. [e] **Pcx-Ge**. [f] **Pcx-Sn**. [g] **Pcx-Pb**. [h] **TS-1a−C**. [i] **TS-1a-Si**. [j] **TS-1a-Ge**. [k] **TS-1a-Sn**. [l] **TS-1a-Pb**. [m] [X−X] stands for $(SiH_3)_2X{-}X(SiH_3)_2$. [n] **Pro-1a−C**. [o] **Pro-1a-Si**. [p] **Pro-1a-Ge**. [q] **Pro-11a-Sn**. [r] **Pro-1a-Pb**. [s] **TS-1b−C**. [t] **TS-1b-Si**. [u] **TS-1b-Ge**. [v] **TS-1b-Sn**. [w] **TS-1b-Pb**. [x] **Pro-1b−C**. [y] **Pro-1b-Si**. [z] **Pro-1b-Ge**. [aa] **Pro-1b-Sn**. [bb] **Pro-1b-Pb**.

> **TS-2a-Br** (+0.19) and **TS-2b-I** (+39) > **TS-2a−I** (−4.1). Likewise, the reaction enthalpy for both reaction pathways is predicted to be the same order (kcal/mol): **Pro-2b-F** (+70) > **Pro-2a-F** (+16), **Pro-2b-Cl** (+20) > **Pro-2a-Cl** (−11), **Pro-2b-Br** (+6.1) > **Pro-2a-Br** (−13) and **Pro-2b-I** (−3.5) > **Pro-2a-I** (−14). Again, these results are consistent with the prediction that the activation barrier should be correlated with the exothermicity of a disilene abstraction.[25]

In brief, the present theoretical study suggests the following about the radical mechanism for the $(SiH_3)_2Si{=}Si(SiH_3)_2 + CY_4$ reaction: First, the reaction rates for $(SiH_3)_2Si{=}Si(SiH_3)_2 + CF_4$ and CCl_4 via both Y-abstraction and CY_3-abstraction routes are expected to be significantly slower than those for CBr_4 and CI_4. In fact, for a given dimetallene, the overall barrier heights are determined to be in the order $CF_4 > CCl_4 > CBr_4 > CI_4$. Namely, the heavier the halogen atom (Y), the more facile is the abstraction of a halogen from CY_4. Second, halogen abstraction is always predicted to be much faster than the abstraction of a CY_3 group.

IV. Overview of Dimetallene Abstraction Reactions

From our survey of the mechanisms of both $(SiH_3)_2X{=}X(SiH_3)_2 + CCl_4$ and $(SiH_3)_2Si{=}Si(SiH_3)_2 + CY_4$ reactions, we come to the following conclusions:

(A) Carbon−halogen activation may proceed via a two-step abstraction-recombination path (formation of the two radicals collapsing in a subsequent step to the final product). This has been confirmed by some experimental observations.[8,9]

(B) In the competition between halogen (Y) and CY_3 abstraction, the latter has the highest energy requirement and the largest endothermicity. As a result, this makes it the least energetically favorable path for dimetallene abstraction. Therefore, halogen abstraction will be the first step in the initial reaction of a dimetallene and a halocarbon and halogen-abstraction products will dominate. Our model conclusions are consistent with some available experimental findings.[8,9]

(C) For a given haloalkane, the more massive and less electronegative the central atoms of a given dimetallene are, the easier the abstraction reaction with haloalkane will be and the larger its exothermicity. That is to say, the reactivity of dimetallenes increases in the order [C=C] < [Si=Si] < [Ge=Ge] < [Sn=Sn] < [Pb=Pb]. More specifically, [Sn=Sn] and [Pb=Pb] can readily abstract halogen atoms from halocarbons, while [C=C] is unreactive toward them.

(D) For a given dimetallene, considering both the activation barrier and reaction enthalpy on the basis of the model calculations presented here, we conclude that the order of reactivity is F ≪ Cl < Br < I. This may be a reflection of carbon−halogen bond strengths (vide infra). That is to say, since the C−F bond has the highest bond energy of the carbon−halogen bonds, it is thus reasonable to predict that the dimetallene should more easily abstract from other carbon−halogen bonds (in particular from C−Br and C−I bonds).

V. Configuration Mixing Model

In this section, an intriguing model for interpreting the relative reactivity of the reactants is provided by the so-called configuration mixing (CM) model, which is based on Pross and Shaik's work.[27] According to the conclusions of this model, the energy barriers governing processes as well as the reaction enthalpies should be proportional to the energy gaps for both dimetallene and carbon tetrahalide; that is, ΔE_{st} ($=E_{triplet} - E_{singlet}$ for $(SiH_3)_2X{=}X(SiH_3)_2$) + $\Delta E_{\sigma\sigma^*}$ ($=E_{triplet} - E_{singlet}$ for CY_4). We thus conclude that both the order of the singlet and triplet states and their energy separation are responsible for the existence and the height of the energy barrier.[27] Bearing these analyses in mind, we shall now explain the origin of the following observed trends:

(1) Why Does the Reactivity of Dimetallene Abstraction Increase in the Order [C=C] < [Si=Si] < [Ge=Ge] < [Sn=Sn] < [Pb=Pb]? According to the CM model discussed above, it is clear that the magnitude of ΔE_{st} for a dimetallene, $(SiH_3)_2X{=}X(SiH_3)_2$, should play a decisive role

(27) (a) Shaik, S. *J. Am. Chem. Soc.* **1981**, *103*, 3691. (b) Shaik, S.; Schlegel, H. B.; Wolfe, S. *Theoretical Aspects of Physical Organic Chemistry*; John Wiley & Sons, Inc.: New York, 1992. (c) Pross, A. *Theoretical and Physical principles of Organic Reactivity*; John Wiley & Sons, Inc.: New York, 1995. (d) Su, M.-D.; Chu, S.-Y. *J. Am. Chem. Soc.* **1999**, *121*, 1045.

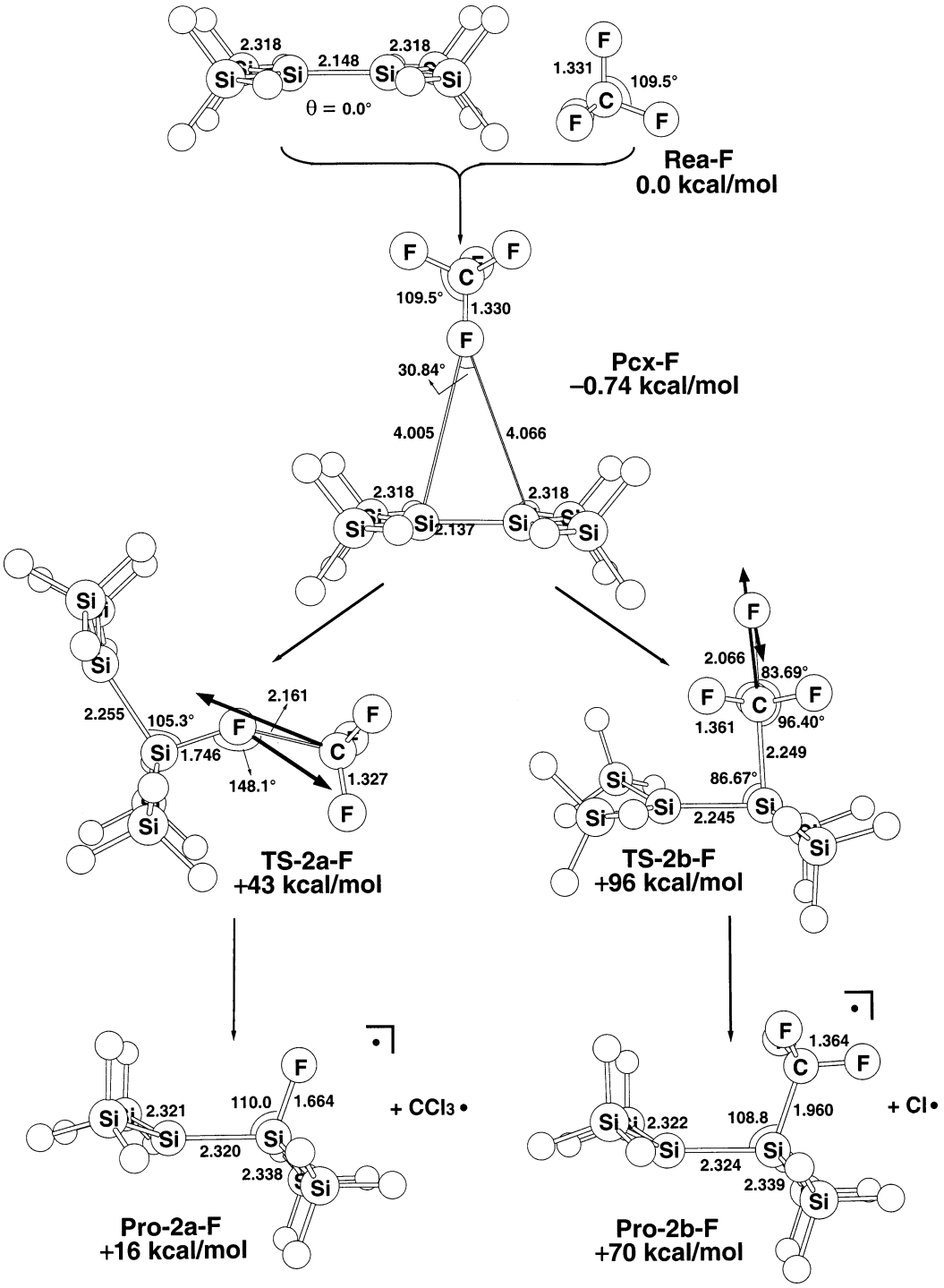

Figure 6. Optimized geometries (in Å and deg) for the reactants (**Rea**), precursor complexes (**Pcx**), transition states (**TSs**), and abstraction products (**Pro**) of $(SiH_3)_2Si{=}Si(SiH_3)_2$ with CF_4 through two reaction pathways (2a) and (2b). All were calculated at the B3LYP/LANL2DZdp level of theory. The heavy arrows indicate the main components of the transition vector. Hydrogens are omitted for clarity.

in determining the reactivity order for dimetallene abstractions. Namely, a smaller ΔE_{st} for the dimetallene molecule results in a lower barrier height and a larger exothermicity. As discussed previously, the reason for the planar to trans-bent distortion in a 12-valence-electron heavy ethylene system is attributed to the second-order Jahn−Teller distortion, the strength of which increases on descending a column in the periodic table;[24] see **3**. As a result, the HOMO−LUMO energy difference for a dimetallene decreases rapidly from carbon down to lead. This, in turn, reduces the dimetallene ΔE_{st} as one proceeds along the series from C to Pb. Indeed, as can be seen in Table 1, our B3LYP results suggest a decreasing trend in ΔE_{st} of $(SiH_3)_2X{=}X(SiH_3)_2$ for [C═C] (36 kcal/mol) > [Si═Si] (21 kcal/mol) > [Ge═Ge] (17 kcal/mol) > [Sn═Sn] (13 kcal/mol) > [Pb═Pb] (11 kcal/mol). This correlates well with the trend in both barrier height and exothermicity, as demonstrated in the previous section.

Furthermore, from a binding energy point of view, it is well-known that the π bond strength of [X═X] decreases from C to Pb.[2k] As a result, the greater the atomic weight of

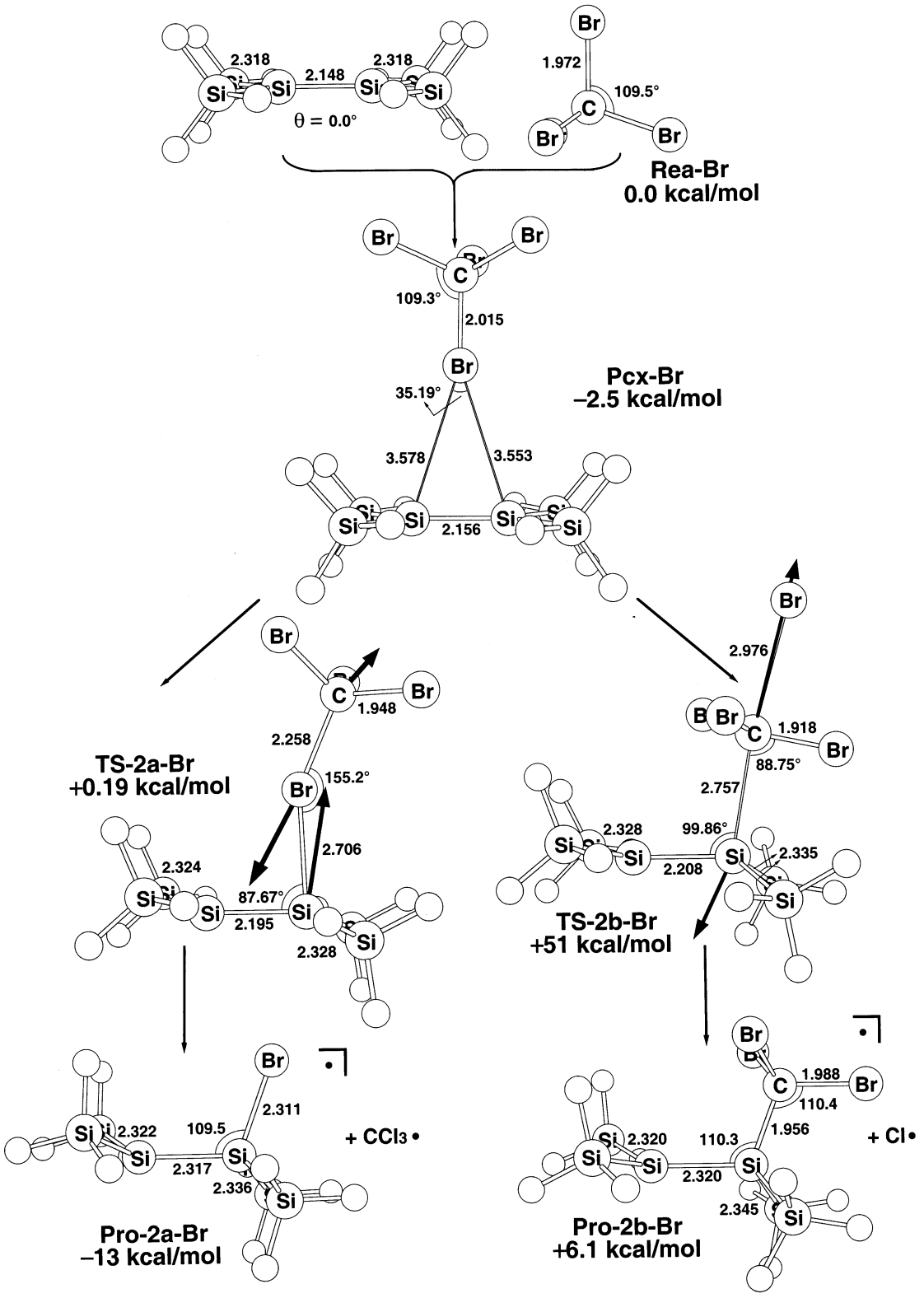

Figure 7. Optimized geometries (in Å and deg) for the reactants (**Rea**), precursor complexes (**Pcx**), transition states (**TSs**), and abstraction products (**Pro**) of $(SiH_3)_2Si{=}Si(SiH_3)_2$ with CBr_4 through two reaction pathways (2a) and (2b). All were calculated at the B3LYP/LANL2DZdp level of theory. The heavy arrows indicate the main components of the transition vector. Hydrogens are omitted for clarity.

X, the weaker the π bond strength of [X=X], the lower its π bond dissociation energy, and the more facile the abstraction reaction becomes. This is indeed observed in this study. Moreover, as can be seen in Table 1, the heavier the main group element, the larger the pyramidalization angle θ (see **1**). This strongly implies that the heavier olefins (in particular for the [Pb=Pb] case) probably have a more significant diradical character,[5b] which can reinforce the abstraction reaction. Consequently, all the above factors suggest that distannene and diplumbene should undergo abstraction reactions with halocarbons much easier than can the corresponding ethylene.

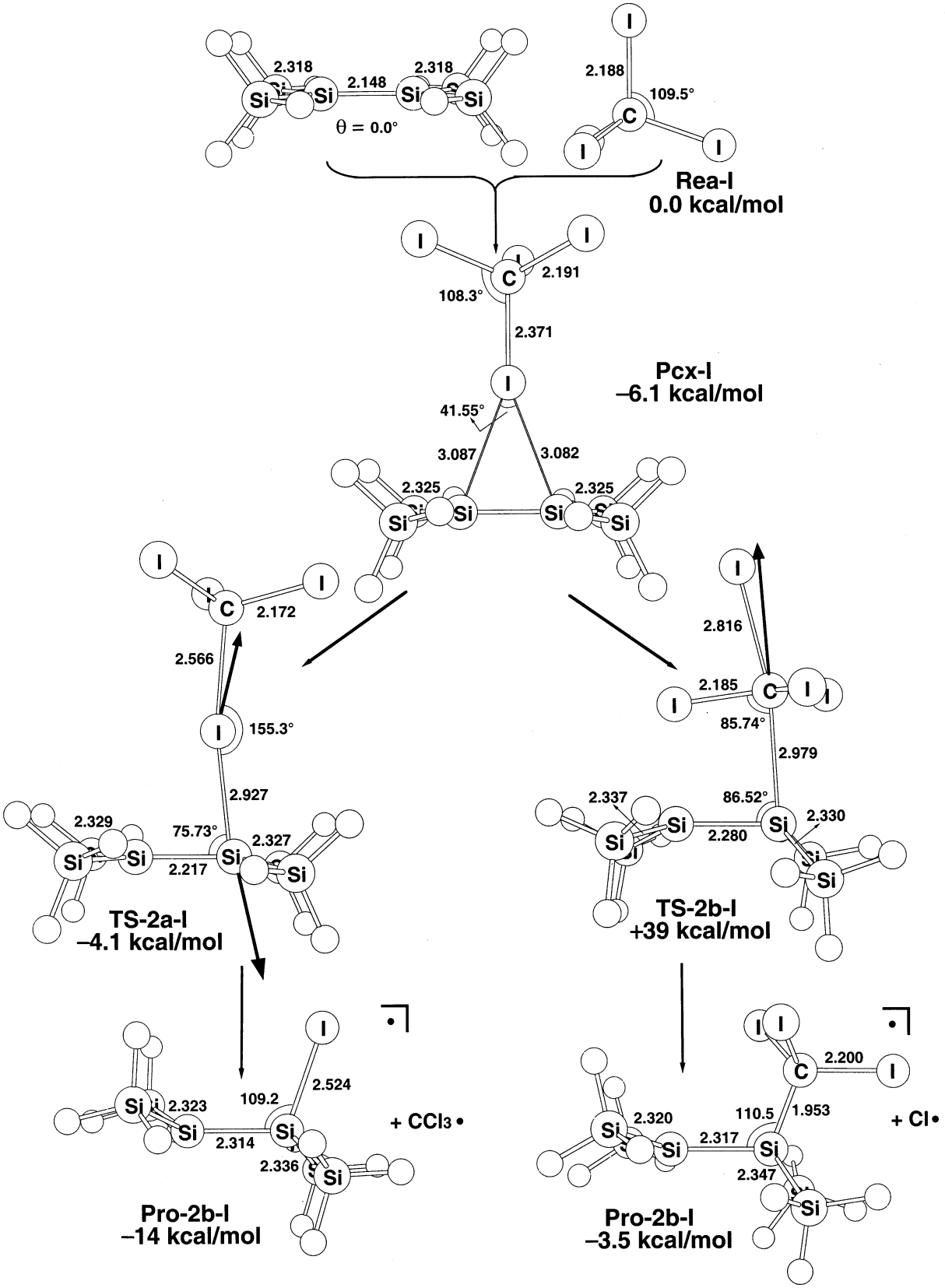

Figure 8. Optimized geometries (in Å and deg) for the reactants (**Rea**), precursor complexes (**Pcx**), transition states (**TSs**), and abstraction products (**Pro**) of $(SiH_3)_2Si{=}Si(SiH_3)_2$ with CI_4 through two reaction pathways (2a) and (2b). All were calculated at the B3LYP/LANL2DZdp level of theory. The heavy arrows indicate the main components of the transition vector. Hydrogens are omitted for clarity.

(2)Why Does the Ease of Halogen Abstraction from CY_4 Increase in the Order C−F < C−Cl < C−Br < C−I? The reason for this can be traced to the singlet−triplet energy gap of carbon tetrahalide (CY_4). That is to say, the smaller $\Delta E_{\sigma\sigma^*}$ for CY_4, the lower the barrier height and the larger the exothermicity, and, in turn, the faster the abstrac-

Table 3. Energies (in kcal/mol) of Stationary Points Relative to the Reactants ($(SiH_3)_2Si{=}Si(SiH_3)_2 + CY_4$, Where Y = F, Cl, Br, and I)[a]

system	Y = F[b]	Y = Cl[c]	Y = Br[d]	Y = I[e]
		Reactants		
$(SiH_3)_2Si{=}Si(SiH_3)_2 + CY_4$	0.0	0.0	0.0	0.0
		Precursor Complex		
	−0.743[f]	−0.520[g]	−2.54[h]	−6.14[i]
		Y Abstraction (Path a)		
transition state	+43.1[j]	+9.96[k]	+0.193[l]	−4.10[m]
$[Si{-}SiY]^{\bullet} + CY_3^{\bullet}$ [n]	+15.5[o]	−10.7[p]	−12.8[q]	−14.0[r]
		CY_3 Abstraction (Path b)		
transition state	+96.3[s]	+60.7[t]	+51.4[u]	+38.6[v]
$[Si{-}SiCY_3]^{\bullet} + Y^{\bullet}$ [n]	+70.0[w]	+19.9[x]	+6.05[y]	−3.49[z]

[a] All at the B3LYP/LANL2DZdp (singlet) or UB3LYP/LANL2DZdp (doublet) levels of theory; see the text. [b] See Figure 6 for structures. [c] See Figure 2 for structures. [d] See Figure 7 for structures. [e] See Figure 8 for structures. [f] **Pcx-F**. [g] **Pcx-Si**. [h] **Pcx-Br**. [i] **Pcx-I**. [j] **TS-2a-F**. [k] **TS-1a-Si**. [l] **TS-2a-Br**. [m] **TS-2a-I**. [n] [Si−Si] stands for $(SiH_3)_2Si{-}Si(SiH_3)_2$. [o] **Pro-2a−F**. [p] **Pro-1a-Si**. [q] **Pro-2a-Br**. [r] **Pro-2a−I**. [s] **TS-2b−F**. [t] **TS-2b-Si**. [u] **TS-2b-Br**. [v] **TS-2b−I**. [w] **Pro-2b-F**. [x] **Pro-2b-Si**. [y] **Pro-2b-Br**. [z] **Pro-2b-I**.

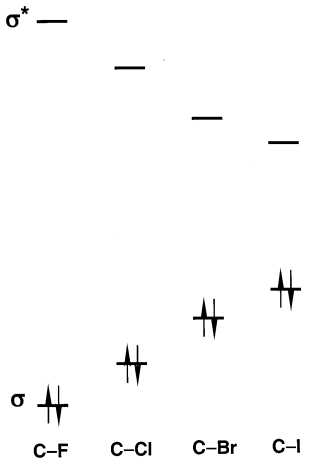

Figure 9. Schematic representation of the relative energy levels for σ and σ^* levels for C−F, C−Cl, C−Br, and C−I bonds. See ref 27c, p 51.

tion reaction. A diagram that illustrates qualitatively the relative σ and σ^* energy levels for the carbon−halogen bonds is shown in Figure 9.[28a] It is evident that the energy of the σ orbitals increases from F to I; that is σ(C−F) < σ(C−Cl) < σ(C−Br) < σ(C−I). On the other hand, the energy of the σ^* orbitals decreases from F to I; that is σ^*(C−F) > σ^*(C−Cl) > σ^*(C−Br) > σ^*(C−I). This strongly implies that the σ(C−Y) → σ^*(C−Y) triplet excitation energy of CY_4 decreases along the series from F to I. Indeed, our DFT calculations[29] confirm this prediction and suggest a decreasing trend in $\Delta E_{\sigma\sigma^*}$ for CF_4 (266 kcal/mol) > CCl_4 (110 kcal/mol) > CBr_4 (73 kcal/mol) > CI_4 (47 kcal/mol).[28b] Namely, the reverse of the order of $\Delta E_{\sigma\sigma^*}$ is the intrinsic reactivity order $F^{\bullet} < Cl^{\bullet} < Br^{\bullet} < I^{\bullet}$. From Table 3, it is readily seen that this result is consistent with the trend in activation energy and reaction enthalpy ($\Delta E^{\ddagger}$, ΔH) for halogen abstraction by $(SiH_3)_2X{=}X(SiH_3)_2$ which are (+43, +15), (+10, −11), (+0.19, −13), and (−4.1, −14) kcal/mol. Likewise, the same explanation can also be applied to the CY_3 abstraction, which follows the same reactivity order as the halogen abstraction reactions as illustrated in Table 3, i.e., $CF_3^{\bullet} < CCl_3^{\bullet} < CBr_3^{\bullet} < CI_3^{\bullet}$. Furthermore, it has been reported that the experimentally determined bond energy for C−F, C−Cl, C−Br, and C−I is 116, 78.2, 68, and 51 kcal/mol, respectively.[30] Again, our theoretical findings are in good agreement with the CM model.

(3) Why is the Halogen (Y) Abstraction Favored over the CY_3 Abstraction for a Given Dimetallene Species? The reactivity order for Y and CY_3 abstractions is explained most probably in terms of the strength of X−halogen vs X−carbon bonds. It was therefore necessary to evaluate the energies of the X−halogen and X−carbon bonds using the B3LYP/LANL2DZdp level of theory presented in this work. To determine the bond energies the series of thermodynamic reactions in eq 3 were used:

$$(SiH_3)_3X{-}Cl \rightarrow (SiH_3)_3X^{\bullet} + Cl^{\bullet} \quad \Delta E_1 \qquad (3a)$$

$$(SiH_3)_3X{-}CCl_3 \rightarrow (SiH_3)_3X^{\bullet} + CCl_3^{\bullet} \quad \Delta E_2 \qquad (3b)$$

$$X = C, Si, Ge, Sn, Pb$$

This series allows for the calculation of the energy difference between the X−Cl and X−C bonds as follows:

$$\Delta E(\mathrm{BDE}) = \Delta E_2 - \Delta E_1 \qquad (4)$$

Our DFT calculations show that the differences in these bond strengths amount to 7.17 (C), 30.3 (Si), 31.0 (Ge), 33.4 (Sn), and 35.4 (Pb) kcal/mol, all being in favor of the X−Cl bonds. Amazingly, this is almost the entire difference in reaction energies between reactions 1a and 1b in Table 2, which are calculated to be 16.0, 30.6, 31.5, 35.5, and 36.1 kcal/mol for [C=C], [Si=Si], [Ge=Ge], [Sn=Sn], and [Pb=Pb] cases, respectively. Accordingly, this provides strong evidence for the fact that the binding energy of X−Cl is much stronger than that of $X{-}CCl_3$ and that $[(SiH_3)_2X{-}X(SiH_3)_2Cl]^{\bullet}$ is more stable than $[(SiH_3)_2X{-}X(SiH_3)_2CCl_3]^{\bullet}$. Likewise, the same argument can also be applied to the $(SiH_3)_2Si{=}Si(SiH_3)_2 + CY_4$ systems as shown in Table 3, which gives a similar conclusion.

VI. Conclusion

In this work, we have studied the mechanisms of dimetallene abstraction reactions with halocarbons by density functional theory. It should be pointed out that this study has provided the first theoretical demonstration of the reaction trajectory and theoretical estimation of the activation energy and reaction enthalpy for these abstraction processes. It should also be emphasized that calculated DFT barrier heights are often, if anything, too low.[31] Thus, those barrier heights quoted here might be underestimated by several kilocalories/mole. It is believed that using more sophisticated theory with larger basis sets is essential to improve these

(28) (a) Reference 27c, p 51. (b) $\Delta E_{\sigma\sigma^*}$ can be evaluated to a good approximation from the energies of the vertical σ(C−Y) → σ^*(C−Y) triplet excitation in CY_4 (Y = F, Cl, Br, and I).

(29) At the B3LYP/LANL2DZ level of theory.

(30) Hueey, J. E.; Keiter, E. A.; Keiter, R. L. *Inorganic Chemistry*, 4th ed.; HarperCollins College Publishers: New York, 1993.

(31) Laird, A.; Ross, R. B.; Zeigler, T. *Chemical Applications of Density Functional Theory*; Americal Chemical Society: Washington, DC, 1996.

estimates.[16] Nevertheless, the energies obtained at the B3LYP/LANL2DZdp level can, at least, provide qualitatively reliable conclusions. Furthermore, we have demonstrated that the computational results can be rationalized using a simple CM model as well as bonding dissociation energies. Thus, not only have we given an explanation for some of the available experimental observations but our approach also provides chemists with important insights into the factors controlling dimetallene abstraction reactions with halocarbons and thus permits them to predict the reactivity of several, as yet unknown, heavier olefinic species.

We encourage experimentalists to carry out further experiments to confirm our predictions.

Acknowledgment. The author is thankful to the National Center for High-Performance Computing of Taiwan and the Computing Center at Tsing Hua University for generous amounts of computing time. He also thanks the National Science Council of Taiwan for financial support. He is grateful to the reviewers for critical comments on the manuscript.

IC0303340